Physica C 470 (2010) 1070–1072

Contents lists available at ScienceDirect

Physica C

journal homepage: www.elsevier.com/locate/physc

Scanning tunneling spectroscopy and break junction spectroscopy on iron-oxypnictide superconductor $NdFeAs(O_{0.9}F_{0.1})$

A. Sugimoto [a,*], T. Ekino [a], R. Ukita [a], K. Shohara [a], H. Okabe [b], J. Akimitsu [b], A.M. Gabovich [c]

[a] Graduate School of Integrated Arts and Sciences, Hiroshima University, Higashi-Hiroshima 739-8521, Japan
[b] Department of Physics, Aoyama Gakuin University, Sagamihara 229-8558, Japan
[c] Institute of Physics, National Academy of Sciences, Nauka Ave. 46, Kyiv 03680, Ukraine

ARTICLE INFO

Article history:
Available online 31 May 2010

Keywords:
Iron-pnictide superconductor
STM
Tunneling spectroscopy

ABSTRACT

Iron-oxypnictide superconductor $NdFeAs(O_{0.9}F_{0.1})$ was studied using both low-temperature scanning tunneling microscopy/spectroscopy (STM/STS) and tunnel break junction (BJ) methods. STM topography showed granular and spot structures with a typical size of several nanometers, most probably governed by fluorine atom distribution. The majority of STS conductance, G, versus voltage, V, curves revealed V-shaped structures, whereas some of $G(V)$ dependences possessed coherent gap peaks or kinks at gap energies. At the same time, $G(V)$ dependences obtained by the BJ technique showed clear-cut coherence peaks with peak-to-peak distances $V_{pp} = 4\Delta/e \sim 25$ mV at 4.2 K, where Δ is the superconducting energy gap, $e > 0$ is the elementary charge. This yields $\Delta(0) = 6$–7 meV, so that the ratio $2\Delta(0)/k_BT_c$ is about 3–4, k_B being the Boltzmann constant. This value is consistent with the conventional weak-coupling s-wave Bardeen–Cooper–Schrieffer theory.

1. Introduction

Recent discovery of iron-pnictide superconductors [1], is of a great importance, because it demonstrated a possibility of new families of materials with T_c's of the same order and even exceeding those of cuprate superconductors. In particular, $LnFeAs(O_{1-x}F_x)$ (Ln: lanthanide) compounds, the so called 1 1 1 1 family, has the highest attained so far T_c of ~55 K among those iron-based materials [2]. It is of value to study superconducting energy gap structures in materials concerned, since they are intimately related to Cooper pairing peculiarities. In this connection, it is especially instructive to examine the above-mentioned family (F-doped 1 1 1 1) with the highest T_c.

Superconducting gaps Δ have been already measured for AFe_2As_2 (A = Ba, Sr, 122 family) [3–5] and $FeSe_{1-x}Te_x$(1 1 family) [6] $SmFeAsO_{0.85}$ (non F-doped 1 1 1 1) [7] using scanning tunnel spectroscopy (STS). The resulting values show that the ratios $2\Delta/k_BT_c$ agree, in general, with the weak-coupling Bardeen–Cooper–Schrieffer (BCS) theory (k_B is the Boltzmann constant). On the other hand, there are only a few STS investigations of the F-doped 1 1 1 1 family [8], probably, because it is difficult to grow corresponding large single crystals.

In this paper, we describe the tunnel spectrum measurements of the polycrystalline iron-oxypnictide superconductor $NdFeAs(O_{0.9}F_{0.1})$ carried out by low-temperature scanning tunneling microscopy/spectroscopy (STM/STS) and tunnel break junction (BJ) methods and compare relevant results.

2. Experimental

Polycrystalline samples were synthesized by heating the mixture of starting material powders in sealed quartz tubes filled with Ar gas at 1500 K during 40 h [1]. $T_c \sim 48$ K was inferred from the temperature, T, dependence of electrical resistance and magnetic susceptibility. The STM equipment used in this experiment is commercially supplied system (Omicron LT-STM) with some modifications [9,10]. Polycrystalline samples were cracked at $T = 77$ K under the ultra-high vacuum atmosphere of $\sim 10^{-8}$ Pa. The Pt/Ir tip was cleaned by high-voltage field emission process with Au single crystal target just prior to STM and STS measurements. STM data were obtained at $T = 4.9$ K under the ultra-high vacuum of $\sim 10^{-8}$ Pa. The conductance curves $G(V_{STS})$ ($G = dI/dV$, where I is the quasiparticle current) were obtained by numerical differentiation of STS current–voltage characteristics.

Tunneling conductance measurements by the BJ method were also carried out for comparison. BJs were formed by cracking the sample at the liquid helium temperature [11]. The conductance curves $G(V_{BJ})$ was measured by an ac modulation technique using a four-probe method in the range $4.2\ \text{K} \leqslant T \leqslant 23$ K.

* Corresponding author. Tel.: +81 82 424 6540; fax: +81 82 424 0757.
E-mail address: asugimoto@hiroshima-u.ac.jp (A. Sugimoto).

0921-4534/$ - see front matter © 2010 Elsevier B.V. All rights reserved.
doi:10.1016/j.physc.2010.05.038

3. Results and discussion

Fig. 1a shows a typical STM image of the NdFeAs($O_{0.9}F_{0.1}$) surface at $T = 4.9$ K. Fig. 1b shows the scanning electron microscope (SEM) image of the same sample taken at room T after the STM observation. Small single crystals of tens of micrometer size are revealed in the SEM image, although the overall sample is polycrystalline. In STM studies, we select such flat surfaces as the observed ones, using the CCD microscope monitor of the STM system to avoid rough and irregular tunneling conditions. Therefore, we managed to hold a stable STM condition, although the sample was a polycrystalline one. STM topography showed randomly distributed granular and spot structures with the typical grain size of several nanometers. A similar topography with randomly distributed granular structures was reported by Pan et al. [8]. We note that random spot structures were also observed in apical fluorine cuprate superconductors [10]. It is quite interesting that such similar spot structures were observed, despite the two different kinds of superconducting system, cuprate and iron-pnictide. The common feature, the existence of "fluorine atoms" in the charge reservoir layer, is considered as one of the origins of such structures.

Measurements of local barrier height (work function φ) by I–z method [9] showed high enough barrier height, $\varphi \sim 4.1$ eV. Additionally, we had confirmed that the tip had the spatial resolution of ~0.2 nm by observing the atomic size structures of gold single crystal during the tip preparation process, indicating that the tunnel conditions in these studies are good enough to ensure the atomic resolution. Nevertheless, the atomic corrugations were not observed. As have been mentioned above, we consider one of the possibilities of the absence of the atomic corrugations is due to some irregular conditions of charge reservoir layers Nd(O, F), which may strongly affect the tunnel current. Fig. 1c shows the averaged conductance $G(V)$ spectrum at $T = 4.9$ K of the whole topographic area depicted in Fig. 1a. The V-shaped $G(V)$ spectra were found for the most of the sample surface (>90%) with no coherence peaks. At the same time, the gap-induced density-of-states (DOS) depletion and traces of gap edges were undoubtedly observed. In iron-pnictide superconductors, such V-shaped conductance spectra were widely reported [3–8].

In Fig. 2, a dashed curve (bottom, blue online) describes the conductance $G(V_{STS})$, which has a gap peak edge at the positive bias. It seems that an existing asymmetric background contribution to the overall $G(V_{STS})$ might prevent distinguishing of the gap edges for negative biases. The gap-peak position is $V_p \sim +8.6$ mV, so that

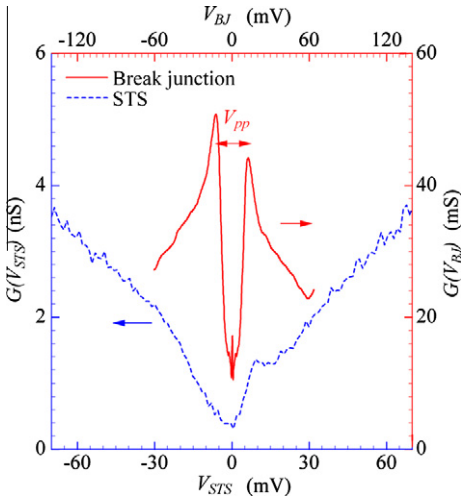

Fig. 2. The conductance spectra $G(V)$ obtained by different methods for NdFeAs($O_{0.9}F_{0.1}$). Dashed line (blue) corresponds to $G(V_{STS})$ for the SIN junction (STS), solid line (red) corresponds to $G(V_{BJ})$ for the SIS junction (BJ). To compare the data, the bias scale for the STS method (SIN junction, V_{STS}) is twice enlarged to match the actual gap values inferred from the BJ spectra (SIS junction, V_{BJ}). (For interpretation of the references to color in this figure legend, the reader is referred to the web version of this article.)

the gap magnitude is Δ_{STS} (4.9 K) ~ 8.6 meV (V_p–Δ_{STS}). This gap agrees with the so-called smaller gap ($\Delta \sim 9$ meV) found in previous reports [8].

Local patterns, displayed in Fig. 1c and the dashed curve in Fig. 2, are very instructive. At the same time, the averaged tunnel measurements are also highly informative. Therefore, we have carried out BJ measurements, in order to clarify the (integrated) macroscopic conductance spectra and to infer the gaps. The solid line in Fig. 2 (top, red online) corresponds to the $G(V_{BJ})$ spectrum obtained by the BJ method. In the case of BJ design, superconductor–insulator–superconductor (SIS) junctions are formed and the relevant peak-to-peak distance V_{pp} corresponds to 4Δ. Therefore, to make a direct comparison the bias voltage axis scale (V_{BJ}) was reduced to half of the scale for the STS measurements (V_{STS}). The bias V_{BJ} is shown at top of the frame. In contrast to the STS spectrum, the BJ conductance curve $G(V_{BJ})$ shows a clear-cut gap-peak feature and is rather symmetric with respect to V_{BJ}. The reason of this success is as follows. In the BJ case, very strong gap-edge peaks and

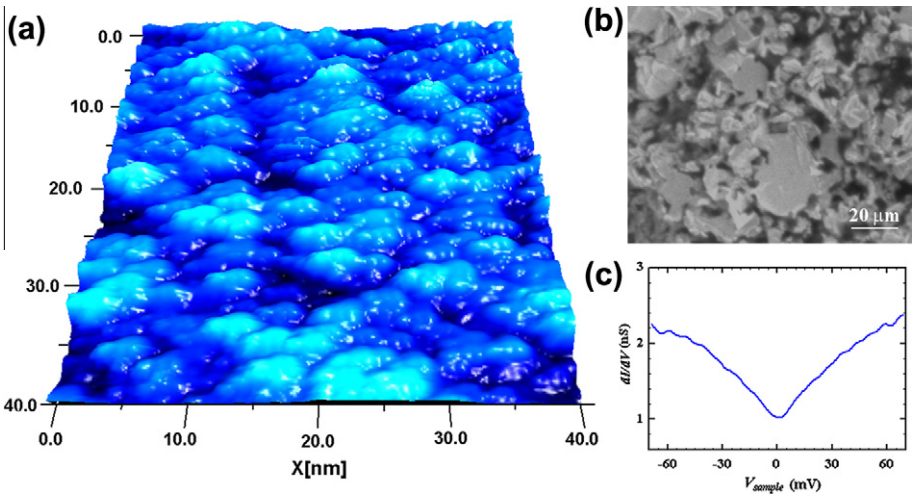

Fig. 1. (a) The typical STM topography on NdFeAs($O_{0.9}F_{0.1}$) ($T = 4.9$ K, $V_{bias} = 0.1$ V, $I_t = 0.25$ nA). (b) SEM image of the same sample as for (a). The white line corresponds to 20 μm. (c) The averaged conductance spectrum $G(V)$ from the whole area of (a).

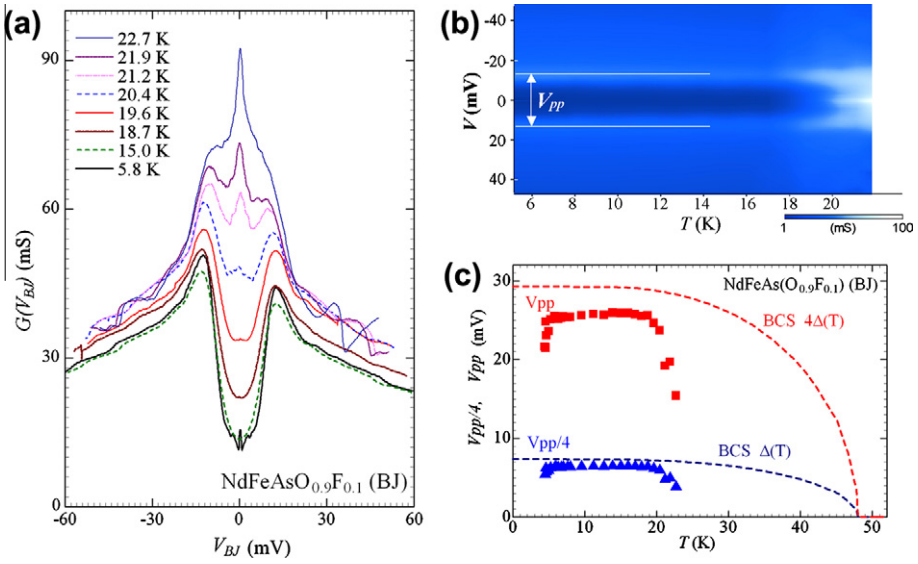

Fig. 3. (a) The temperature, T, dependence of $G(V)$ obtained by the BJ method (5.5 K $\leqslant T \leqslant$ 23 K). (b) Colored-top view of the T–V diagram for $G(V)$. The magnitude of $G(V)$ is represented by the gradation contrast scale. (c) The peak-to-peak voltage V_{pp} and $V_{pp}/4$ temperature plots obtained from the spectrum curve from (a). (For interpretation of the references to color in this figure legend, the reader is referred to the web version of this article.)

well-depressed intra-gap floor should be observed, because the relevant dI/dV is a convolution of two singular superconducting DOSes. The revealed peak-to-peak voltage V_{pp} is about 25.3 mV, so that the estimated gap is $\Delta_{BJ} \sim 6.3$ meV, if we assume $V_{pp} = 4\Delta_{BJ}$. This value is slightly lower than that found in our STS measurements (74%), but it is in a qualitatively good agreement with the latter. Thus, the gap edge value found by the STS is confirmed by the BJ method.

Fig. 3a shows the T dependence of the conductance spectra (5.8 K $\leqslant T \leqslant$ 22.7 K) obtained by the BJ method on the same NdFeAs($O_{0.9}F_{0.1}$) sample as that analyzed in Fig. 1. Because the junctions are of the SIS type, there are zero-bias peaks in some spectra, which may due to the Josephson effect and/or a leak current between grain boundaries. The measurement for $T > 23$ K could not be carried out because the configuration of the junction varied with temperature. Fig. 3b shows the (colored online) T–V diagram of the conductance spectra. The series of $G(V)$ data is same as in Fig. 3a. Bright contrast line areas correspond to the gap peaks and V_{pp} is indicated by the arrow. We can easily see that the spectra and the gap-peak positions almost do not change with T until about ~18 K, and the V_{pp} is reduced around 20 K. At present, we consider the reducing of V_{pp} around 20 K is mainly due to the change of the configuration of boundaries at junction caused by thermal effect, and/or the existence of the lower-T_c areas just at the junction. Fig. 3c shows the peak-to-peak voltage $V_{pp}(T)$ plot obtained from the data displayed in Fig. 3a, accompanied by a corresponding $V_{pp}(T)/4$ curve to compare with theoretical $\Delta(T)$. Dashed lines are weak-coupling s-wave BCS curves with $T_c = 48$ K. The magnitude of the gap $\Delta(T)$ is a constant value of 6–7 meV up to 20 K. Therefore, the zero-T gap magnitude $\Delta(0)$ is estimated as ~6.5 meV, so that the ratio $2\Delta(0)/k_BT_c$ is about 3.2. This value is consistent with the conventional s-wave BCS constant (≈3.52). The gap magnitude obtained agrees well with the gap found for the Γ-point of the Fermi surface as reported by angle-resolved photoemission (ARPES) measurements [12]. However, our experiments, whatever the temperature, did not reveal a multiple-gap spectrum, corresponding to the multiple-pocket Fermi surface, which was observed in the cited ARPES studies. It might happen that the predominantly double-gap structure, if any, has not been resolved, since the BJ spectra constitute a real-space averaged information.

4. Summary

The tunnel spectrum experiments in the iron-oxypnictide superconductor NdFeAs($O_{0.9}F_{0.1}$) were carried out by using both the low-temperature scanning tunneling microscopy/spectroscopy (STM/STS) and the tunnel break junction (BJ) method. Both kinds of data were compared. The gap value inferred by the STS is $\Delta(4.9\text{ K}) = 8.6$ meV, while that found by the BJ method is smaller, namely, $\Delta(0) = 6.5$ meV. In both cases, the ratio $2\Delta(0)/k_BT_c$ is about 3–4, which is consistent with the conventional weak-coupling s-wave BCS theory.

Acknowledgements

We thank the Natural Science Center for Basic Research and Development, Hiroshima University for supplying liquid helium. This research was supported by Grant-in-Aid for Scientific Research (No. 19540370) from JSPS, Japan. A.M.G. highly appreciates the 2009 Visitors Program of the Max Planck Institute for the Physics of Complex Systems (Dresden, Germany).

References

[1] Y. Kamihara, T. Watanabe, M. Hirano, H. Hosono, J. Am. Chem. Soc. 130 (2008) 3296.
[2] Z.-A. Ren, J. Yang, W. Lu, X.-L. Shen, Z. Cai Li, G.-C. Che, X.-L. Dong, L.-L. Sun, F. Zhou, Z.-X. Zhao, Europhys. Lett. 82 (2008) 57002.
[3] F. Massee, Y. Huang, R. Huisman, S. de Jong, J.B. Goedkoop, M.S. Golden, Phys. Rev. B 79 (2009) 220517(R).
[4] M.C. Boyer, Kamalesh Chatterjee, W.D. Wise, E.W. Hudson, Cond-mat. 0806.4400.
[5] Yi Yin, M. Zech, T.L. Williams, X.F. Wang, G. Wu, X.H. Chen, J.E. Hoffman, Phys. Rev. Lett. 102 (2009) 097002;
Yi Yin, M. Zech, T.L. Williams, J.E. Hoffman, Physica C 469 (2009) 535.
[6] T. Kato, Y. Mizuguchi, H. Nakamura, T. Machida, H. Sakata, Y. Takano, Cond-mat. 0910.1485.
[7] O. Millo, I. Asulin, O. Yuli, I. Felner, Z.-A. Ren, X.-L. Shen, G.-C. Che, Z.-X. Zhao, Phys. Rev. B 78 (2008) 092505.
[8] M.H. Pan, X.B. He, G.R. Li, J.F. Wendelken, R. Jin, A.S. Sefat, M.A. McGuire, B.C. Sales, D. Mandrus, E.W. Plummer, Cond-mat. 0808.0895.
[9] A. Sugimoto, T. Ekino, H. Eisaki, J. Phys. Soc. Jpn. 77 (2008) 043705.
[10] A. Sugimoto, K. Shohara, T. Ekino, Y. Watanabe, Y. Harada, S. Mikusu, K. Tokiwa, T. Watanabe, Physica C 469 (2009) 1020.
[11] T. Ekino, T. Takabatake, H. Tanaka, H. Fujii, Phys. Rev. Lett. 75 (1995) 4262.
[12] H. Takahashi, K. Igawa, K. Arii, Y. Kamihara, M. Hirano, H. Hosono, Nature 453 (2008) 376.